Glass fibre composite elements with embedded fibre Bragg grating sensors inspected by THz spectroscopy

Magdalena MIELOSZYK[*,1], Katarzyna MAJEWSKA[1], Wieslaw OSTACHOWICZ[1,2]

[1] Institute of Fluid Flow Machinery of PASci, Fiszera 14, 80-952 Gdansk, Poland, mmieloszyk@imp.gda.pl
[2] Warsaw University of Technology, Narbutta 84, 02-524 Warsaw, Poland

Abstract
Composite materials are very popular in many branches of industry like aerospace, automotive, marine etc. From the Structural Health Monitoring point of view it is very important to know the internal strain of the element during its exploitation. One of the options is development of composite elements with fibre optic sensors embedded during manufacturing process. It is possible due to small size, weight and high multiplexing capabilities of fibre optics sensors (e.g. fibre Bragg grating sensors).
One of t*he problems for such smart structures is discontinuity in the element's material* structure on a boundary between fibre optic and matrix. Such problem can be a result of fault *during manufacturing process as well as can occur during element's exploitation.* The discontinuities can result in damage occurrence (e.g. delamination) that significantly decreasing element strength. So it is important to have a method to inspect the internal structure of the element just after manufacturing process and during its exploitation. On the other hand for painted element with embedded fibres is hard to determine sensors *localisation between layers without having element's geometrical specification.*
The paper presents an application of THz spectroscopy for observation and evaluation the internal structure of glass fibres reinforced composite samples with embedded fibre Bragg grating sensors. The experimental investigation is performed on rectangular samples with four layers manufactured during infusion process. In every sample two fibre Bragg grating sensors with different grating length are embedded.

Keywords: THz spectroscopy, glass fibre composite, fibre optic, Structural Health Monitoring

1. INTRODUCTION

In recent years, composite materials have been widely used in many industrial branches like aviation [13], marine [10] and civil engineering [3]. The composite structures are working in different environmental conditions (harsh due to weather condition, changes in working temperature range, loading, radiation etc.) so ensure their reliability is important to guarantee safety of people and ecosystems. One of the most popular solution are structural health monitoring (SHM) systems permanently installed on civil engineering [3], [4], [14] or marine [10] structures. Among many systems those based on embedded Fibre Bragg Grating (FBG) sensors become more and more popular [11], [12]. FBG sensors have small size and weight, multiplexing capabilities, immunity to electromagnetic fields, high corrosion resistance and require no calibration [5], [6]. Due to their advantages they can be embedded in composite material element during manufacturing process. One of the problem that can occur is discontinuity in the composite material element on boundary between fibre optic and matrix. This can result in damage occurrence (e.g. delamination) significantly decreasing element strength.

The internal structure of a composite element can be inspected using different techniques based on electromagnetic radiation. Spectral range of electromagnetic radiation due to interaction between electromagnetic wave and material structure as well as applications of the waves being a results of their behaviour is divided into several ranges. One of the most interesting ones are THz waves. The typically frequency range is from 0.1 THz to 10 THz. The wavelengths that are related to the THz waves are in a range of 3 mm to 30 μm. It is worth mention that power generated by THz beam is very low and typically the mean power is below 1 μW [7] so risk of destroying sensitive materials is strongly limited [1].
THz radiation can be used in analysis of materials that affects minimum one of three THz wave parameters: refractive index, absorption coefficient or wave scattering referred to roughness of the material surface. This technique cannot be used for internal inspection of conductive material like metals [2]. The THz technique working both in transmission and reflection mode has unique capacity for examining composite materials and identification of defects like gaps, delaminations, mechanical damage or burning on the material surface [9].
The paper presents possibility of application of THz spectroscopy for determination localisation of fibre optics with fibre Bragg grating sensors embedded in glass composite material elements. The experimental investigation is performed on rectangular samples with four layers manufactured using infusion process. In every sample two fibre Bragg grating sensors with different grating length are embedded.
The paper is organised as follow. Firstly glass fibre reinforced polymer (GFRP) samples with embedded FBG sensors are described. Then the THz spectroscopy analysis results for the samples are presented. The limitations of the method are also presented and discussed. At the end some conclusions are drawn.

2. EXPERIMENTAL INVESTIGATION

The measurements were performed on rectangular GFRP samples in a dimension of 70 mm x 200 mm x 1.6 mm. Every sample has four layers and two fibre optic with FBG sensors embedded between 1st and 2nd layer counting form the bottom of the sample. The laminates were manufactured using infusion method for bidirectional material (glass SGlass®) and epoxy resin. During preparation process the material was laying on a metal plate covered by PTFE layer allowing easy removing sample. The material plies were covered by additional material layer in a purpose of an equal distribution of the resin during the manufacturing process. Due to this the bottom surface of every sample is smooth while the top one is rough. The physical parameters of a glass material and bare fibre optic are similar. The main difference is that the glass fibres are intertwined making one textile while fibre optics is separated. The dimension of fibre optics is about 0.250 mm and is smaller than the thickness of textile (0.400 mm) used for making one layer of the composite sample.
The internal structure of the composite samples was examined using THz spectrometer (TPS Spectra 300 THz Pulsed Imaging and Spectroscopy from TerraView®) in reflection mode (Figure 1). In that case the measuring heads are arranged in a angle of 22° between them. The system contains scanning unit (Gantry Imaging system) with moving platform that allows to scanning chosen area of samples. During all measurements the measurement step was equal to 0.2 mm. All measurements were performed with 25 averaging.
As the THz waves are sensitive on moisture in the ambient all measurements were performed with air dryer that removes moisture from the working heads area and air condition that stabilise laboratory temperature on assumed level equal to 20°C.

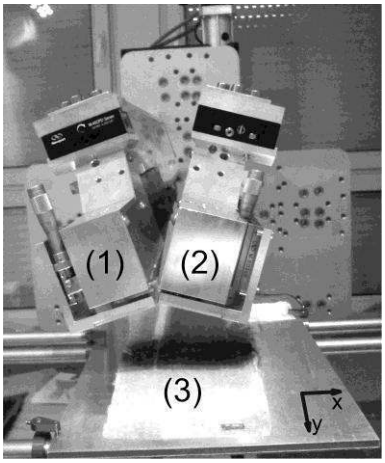

Figure 1. THz spectrometer in the reflection mode: (1) – emitting head, (2) – receiving head, (3) GFRP sample on a metal table.

During the experimental investigation differences in interaction between THz wave and fibre optic embedded into material or lying on a sample surface were compared.
From a variety of measurements two cases are presented and discussed in the paper. In the first one embedded fibres are parallel to the y axis (Figure 1) of the spectrometer, while in the second case the fibres are perpendicular to the y axis.
The pulsed THz spectroscopy method allows to present achieved data using few imaging techniques defined as A-scan, B-scan and C-scan. A-scan is a signal received after measurements of THz wave interaction with analysed material in one point. The signal shape is a combination of all pulses reflected from every boundary between mediums that reached the receiver with optical time delay referred to refractive index of mediums where the THz wave propagates. The measured THz signal shape is also affected by absorption coefficient that change the signal amplitude. An analysed sample surface roughness also affect the received signal by changing its amplitude and time delay. Amplitude, period and time differences between pulses in received THz signal gives information about internal structure of analysed material.

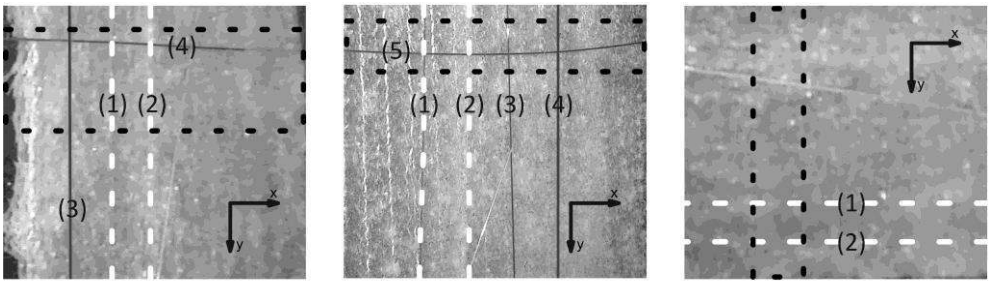

Figure 2. Three (a), (b), (c) GFRP samples with fibre optics: embedded into material structure (1), (2) and lying on the samples' surfaces (3)–(5).

B-scan is a set of signals measured for points (A-scan) lying on chosen line. This representation allows to observe internal structure of the analysed sample. Collecting A-scans for all points of the analysed sample in similar way it is possible to create 3D matrix that can be cut for specific time delay. C-scan is a map presenting signal amplitudes for all points for chosen time delay. If the refractive index of top sample parts are similar for whole analysed sample it allows to present structure of the material on chosen sample thickness. For all

analysed cases the achieved results are presented as B-scans and C-scans.
The sample photographs with marked rectangular scanning areas (black dashed lines) are presented in Figure 2. They contains GFRP material with embedded fibres (denoted as (1) and (2) – white dashed lines) and fibres put on the samples' surfaces (denoted as (3) – (5) – grey solid lines). Additionally the axis directions referred to THz spectrometer are also presented in the photographs.

2.1 First Measurement Case

The first measurement case was performed for samples (Figure 2 (a) and Figure 2 (b)) with embedded fibres parallel to the y axis of the THz spectrometer. For that case an influence of surfaces roughness on THz imaging are presented.

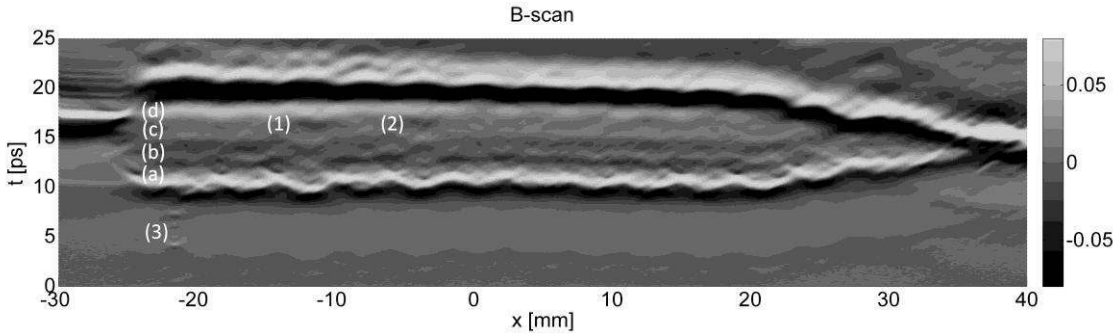

Figure 3. B-scan from the rough side of the sample; (a)–(d) composite layers; (1) and (2) – embedded fibres, (3) fibre lying on the sample surface.

The first measurement was performed from the rough (top surface) side (Figure 2(a)). The scanning rectangular area (with a dimension of 70 mm x 10 mm) contains GFRP material with fibres and a part of the metal table. During this measurement the fibres were embedded between 3rd and 4th layer of the sample counting from top.

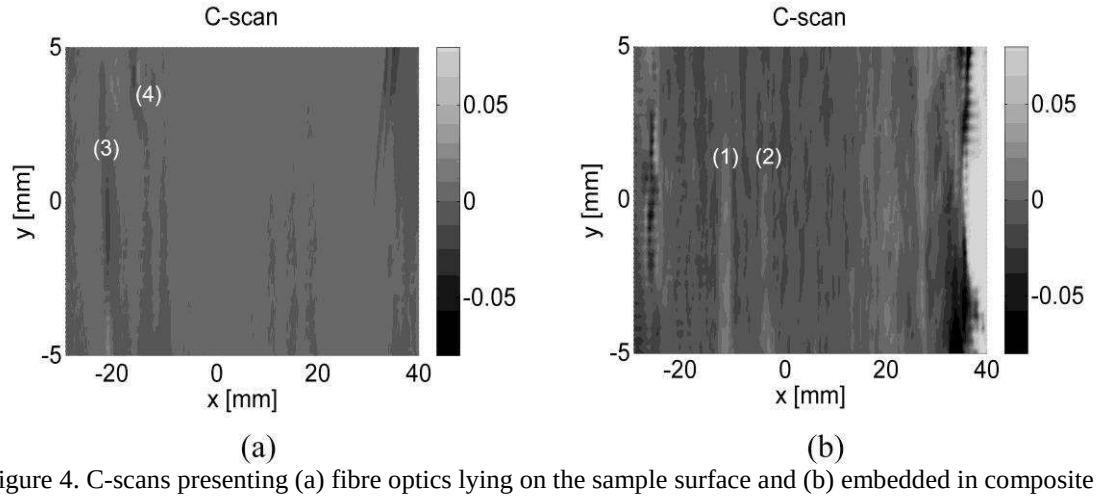

Figure 4. C-scans presenting (a) fibre optics lying on the sample surface and (b) embedded in composite material; (1) and (2) – embedded fibres, (3) and (4) fibres lying on the sample surface.

The sample do not have stable thickness for whole dimension that is especially visible between 20 mm and 40 mm on x axis direction where the sample is visibly thinner. For the rest of the sample its thickness is stable and the number of layers (4) can be easily determined. The sample structure for a part with embedded fibres and one fibre (denoted as

(3)) lying on the sample surface (y= -4.2 mm) is presented as a B-scan in Figure 3. Locations of the fibres in the sample thickness direction can be easily determined, because they are visible as disturbances having dimension of fibre optics and ending at a particular fibre location. For fibres lying on the surface the first reflections from the fibres are visible on a distance of t= 5 ps before the wave reaches the sample and on its surface. For embedded fibres they are visible on the sample surface as a circular disturbance that is ending at the fibres location – between 3rd and 4th layer of the sample.
Two C-scans for the sample are presented in Figure 4. The first one (Figure 4(a)) made for t= 7.5 ps presents sample surface where parallel fibre (denoted as (3)) lying on the sample is well visible. The perpendicular fibre (denoted as (4)) is visible only in locations when it is crossing another fibre. The disturbances on the reflection from the sample surface being an influence of embedded fibre optic are slightly visible on the fibres locations but they are similar to those originated from sample surface pattern. The second C-scan is made for embedded sensors location (t= 14.7 ps). The embedded fibres (denoted as (1) and (2)) are well visible as straight lines.

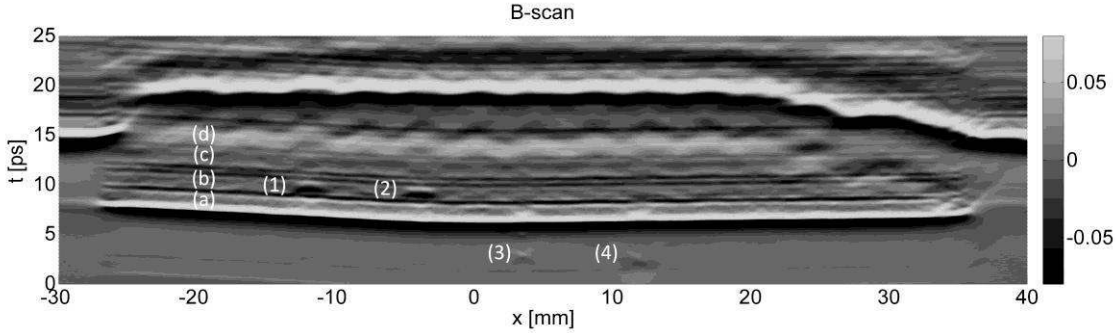

Figure 5. B-scan for the smooth side of the sample; (a)–(d) composite layers; (1) and (2) – embedded fibres, (3) and (4) fibres lying on the sample surface.

The next measurement was performed from the smooth (bottom surface) side – Figure 2(b). The scanning area had a dimension of 70 mm x 5 mm and also contains whole sample width and a small part of the metal table.

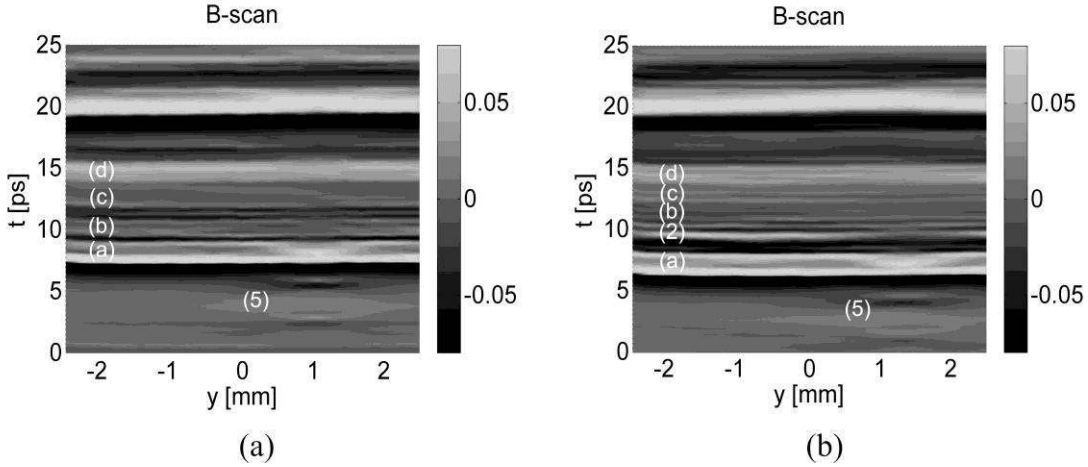

Figure 6. B-scans presenting material structure: (a) without embedded fibre, (b) with embedded fibre; (a)–(d) composite layers; (2) – embedded fibre, (5) fibre lying on the sample surface.

The sample also do not have a stable thickness for whole dimension. The sample internal structure is presented in B-scan (Figure 5) made for a place where only fibre optics parallel to y axis direction are visible (y= -2.1 mm). All fibre optics can be easily determined. The fibres lying on the sample surface are visible as a disturbance about 3 ps, while the embedded on t= 11 ps. For the fibres lying on the surface the absorption (scattering, damping) effect is not as much visible as for embedded fibres. The "trace" visible in the sample depth direction (t axis) after embedded fibres is wider than for the ones lying on the sample surface.
A comparison of two B-scans performed parallel to the embedded fibres is presented in Figure 6. The first one (Figure 6(a)) was made for the material only (x= -17.2 mm) while the second one (Figure 6(b)) for a part with embedded fibre (denoted as (2)) for x= -3.9 mm. In both scans it is also possible to determine thickness of every layer of the composite material. In both B-scans the fibre (denote as (5)) lying on the sample surface parallel to the x axis is well visible as an disturbance starts at t= 2.0 ps and on the first layer of the sample (denoted as (a)). For the second B-scan (Figure 6(b)) the fibre optic is well visible as straight stripe between layers denoted as (a) and (b). On the area of crossing paths of those two fibres denoted as (2) and (5) is harder to determine the fibre dimension because a part of the THz wave was reflected from the fibre denoted as (5) lying on the sample surface and do not propagate into material depth.

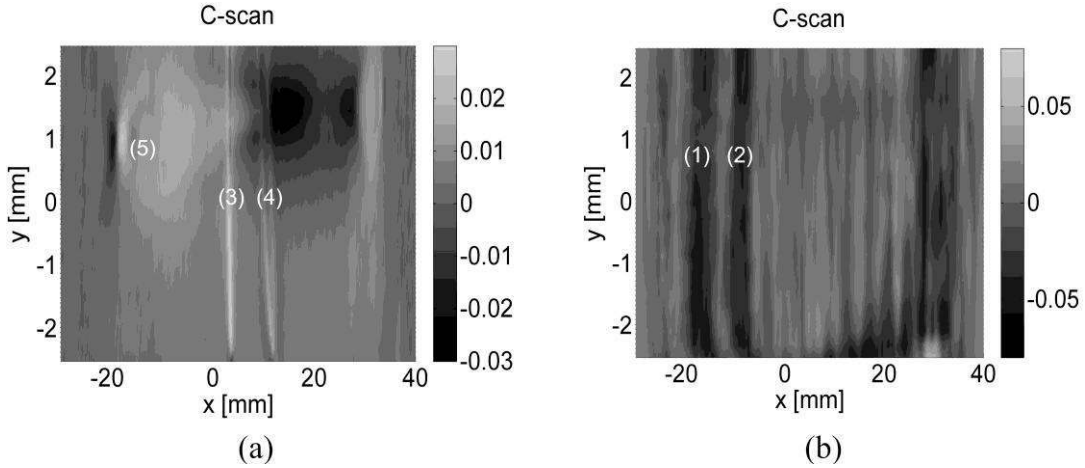

Figure 7. C-scans presenting (a) fibre optics lying on the sample surface and (b) embedded in composite material; (1) and (2) – embedded fibres, (3)–(5) fibres lying on the sample surface.

Two C-scans for the sample with embedded FBG sensors are presented in Figure 7. The first one (Figure 7(a)) made for t= 3.0 ps presents sample surface where parallel fibres (denoted as (3) and (4)) lying on the sample are well visible. The perpendicular fibre (denoted as (5)) is visible only in locations when it is crossing another fibre even embedded in the structure. The disturbances on the sample surface being an influence of embedded fibre optic are visible only close to the fibre optic lying on the sample surface parallel to the x axis. The second C-scan (Figure 7(b)) was made for embedded sensors location (t= 11.0 ps). The embedded fibres (denoted as (1) and (2)) are well visible as straight lines. In this case the distance between sample surface and fibres equal to one layer are smaller than for the previous case where it was equal to 3 layers. So in the case (Figure 7(b)) the amplitudes of the reflected THz waves are almost equal for whole examined fibre optic length, in the previous one (Figure 4(b)) the achieved values slightly differ due to locally varying thickens due to unequally distributed epoxy to every layer of the sample.

2.2 Second Measurement Case

The second measurement case was presented for the sample (Figure 2(c)) with embedded fibres lying parallel to the x axis of the THz spectrometer. The analysed sample contains also 4 layers and the fibres optic embedded between 3rd and 4th layer. The measurement was performed from the rough side. The scanning rectangular area had a dimension of 45 mm x 65 mm and contains GFRP material part with embedded sensors (denoted as (1) and (2)).

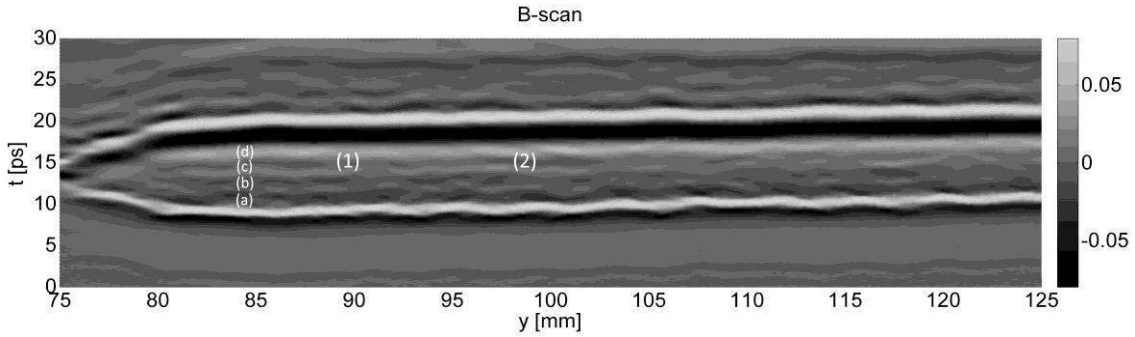

Figure 8. B-scan for the sample with FBG sensors lying parallel to the x direction;
(a)–(d) composite layers; (1) and (2) – embedded fibres.

The B-scan for x= 70.1 mm for the third sample is presented in Figure 8. The sample layers are well visible despite of an influence of unequal resin distribution during sample preparation process. The embedded fibres (denoted as (1) and (2)) can be determined as ends of disturbances that can be observed from the sample surface. A part of B-scan focusing on a part of the sample with fibre optic is presented in Figure 9(a). Due to smaller scale range the determination of localisation of the fibre optics is easier but in a comparison with fibres (Figure 3) lying perpendicular to the x axis of the THz unit the ones lying parallel are less visible.

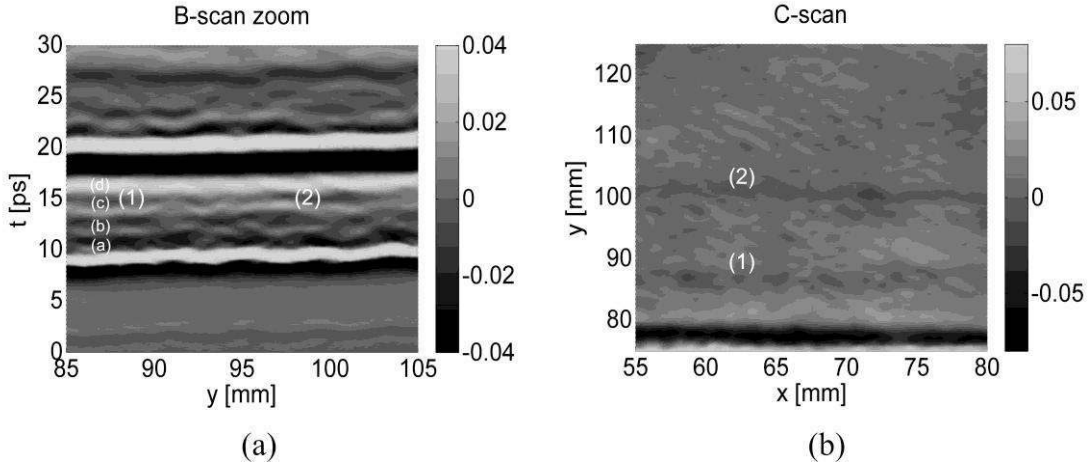

Figure 9. Sample with optic fibres lying parallel to the x direction of the THz unit: (a) B-scan with a part of the sample with embedded optic fibres, (b) C-scan presenting fibres embedded in composite material;
(a)–(d) composite layers; (1) and (2) embedded fibres.

Similar problem of sensitivity level is observed on C-scan (Figure 9(b)) performed for time delay equal to the moment when THz wave reach the fibre optics (t= 16.0 ps). In comparison with previously presented C-scans (Figure 4(b) and Figure 7(b)) performed for fibre optics lying perpendicular to the x axis direction the detection/localisation of fibre optics is much more harder.

3. INTERACTION BETWEEN THZ WAVE AND CIRCULAR FIBRE OPTIC

The results presented above shows that it is possible to distinguish fibre optics lying on a sample surface and embedded in the structure of composite material despite of its position according to the x axis direction (parallel, perpendicular). It is also possible to determine localisation of embedded fibres in the sample thickness direction. However in both cases it is easier to recognise fibres lying parallel to the y direction of the THz spectrometer than perpendicular to it (see Figure 1).

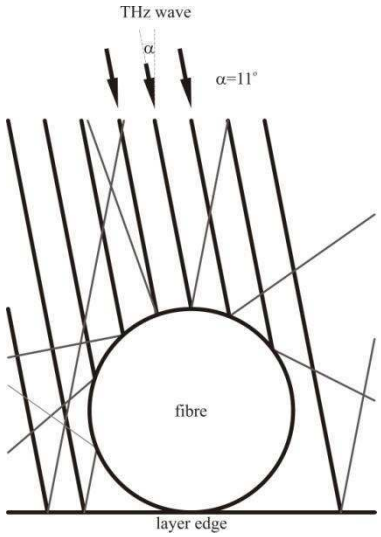

Figure 10. Schema of THz wave interaction with circular fibre parallel to the y axis of the THz unit.

Due to geometrical characterisation of a fibre optic (circular cross-section) the THz wave is partially scattered on it. Only a part of the wave reflected from the fibre can reach the detector. Analogical effect is visible for embedded fibres but surrounding material also interact with the THz wave. The schema of interaction between THz wave and circular fibre lying parallel to the y axis of the THz unit is presented in Figure 10. As it is visible due to the fibre cross-section shape many of the THz waves that are reflected do not have even a chance to reach receiver head. The problem is much more harder when the fibre is parallel to x axis of the THz unit. As it is presented in Figure 1 the scanning heads are lying in one line perpendicular to the metal table. So, when the THz waves from the emitter reach a fibre lying perpendicular to the y axis the majority of them are reflected in planes with different angles not equal to the one for the scanning heads. In that case the waves reflected from the fibre lying on the surface are not detected and waves that reach the composite material have strong chance to be trapped by the fibre in the composite material. On the other side leaving composite they can be also reflected in directions that do not allow to reach the receiver head. Despite of this inconvenience it is possible to determine thickness of a fibre optic using THz spectrometer and according to the experimental investigation the measurement error of determination the fibre optic thickness is between 0.14 to 5%.

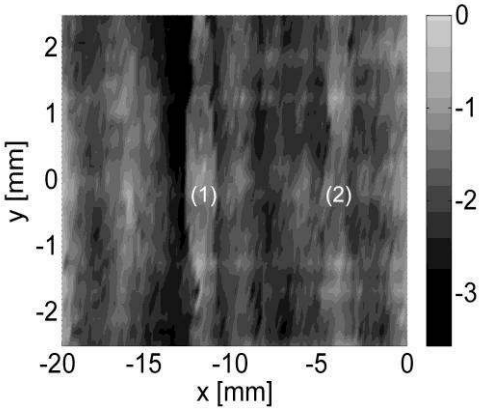

Figure 11. Map originated from deconvolution method presenting location of embedded fibre optics in sample (Figure 2 (a)); (1) and (2) embedded fibres.

The specific behaviour of fibre optics described above allows to use filtering methods for determination of their location in xy plane. One of them is a deconvolution method in a frequency domain. The deconvoluton was calculated in Matlab environment according to an equation

$$[q, r] = deconv(v, u) \quad (1)$$

where q means quotient, r – remainder, v – THz signal measured in the sample, u – THz impulse reflected from a mirror. A map made out of the quotient values q shows fibre optics location (Figure 11). An advantage of this method is a possibility of determination of localisation of fibre optics in xy plane without analysing B- and C-scans manually. Although fibres location in thickness direction (z) still needs consecutive analysis of B-scans made for lines of points that are chosen based on the q-map.

CONCLUSIONS

It is possible to localise glass fibre optics with fibre Bragg grating sensors embedded in a glass fibre composite material as well as fibres lying on the sample surface using THz spectrometry technique. The proposed method can be used to distinguish those two glass fibre optics localisations despite the material parameters of all examined elements are similar. The THz wave is affected mostly by changes of refractive index of analysed material and its absorption coefficient. Additionally there is a problem of scattering occurs for both rough sample surface as well as circular shape of a fibre optics. Although the influence of the second factor is much more harder than of the previous one. Despite of this inconvenience it is possible to determine thickness of a fibre optic using THz spectrometer and the achieved measurement's error is not higher than 5%.

An application of a deconvolution method for fibre optics localisation in xy plane is also presented. The main advantage of this method is a possibility of finding the fibres without knowing their position in the sample.

ACKNOWLEDGEMENTS

This research was supported by the project entitled: Non-invasive Methods for Assessment of Physicochemical and Mechanical Degradation granted by National Centre for Research and Development in Poland - Project No. PBS1/B6/8/2012.

REFERENCES

[1] Cai Y., Brener I., Lopata J., Wynn J., Pfeiffer L., Federici J., Design and performance of singular electric field terahertz photoconducting antennas. Appl. Phys. Lett. **71**, 2076-278, 1997.

[2] Chan W.L., Deibel J., Mittleman D.M., Imaging with terahertz radiation, Rep. Prog. Phys., **70,** 1325–1379, 2007.

[3] Gebremichael YM, Li W, Boyle WJO, Meggitt BT, Grattan KTV, McKinley B, Fernando GF, Kister G, Winter D, Canning L, Luke S, Integration and assessment of fibre Bragg grating sensors in an all—fibre reinforced polymer composite road bridge. Sensors Actuators A, **118,** 78–85, 2005.

[4] Li D., Zhou Z., Ou J., Dynamic behavior monitoring and damage evaluation for arch bridge suspender using GFRP optical fiber Bragg grating sensors. Optics & Laser Technology, **44,** 1031–1038, 2012.

[5] Li H.N., Li D.S., Song G.B., Recent applications of fiber optic sensors to health monitoring in civil engineering. Eng Struct., **26,** 1647–57, 2004.

[6] Majumder M., Gangopaadhyay T.K., Chakraborty A.K., Dasgupta K., Bhattacharya D.K., Fibre Bragg gratings in structural health monitoring-present status and applications. Sens Actuators A Phys., **147,** 150–64, 2008.

[7] Mittleman D., Terahertz Imaging, (in) Daniel Mittleman (Ed.), Sensing with Terahertz Radiation, Springer-Verlag Berlin Heidelberg, 2003.

[8] Redo-Sanchez A., Laman N., Schulkin B., Tongue T., Review of Terahertz Technology Readiness Assessment and Applications. J Infrared Milli Terahz Waves, **34**, 500–518 2013.

[9] Stoik C.D., Bohn M.J. Blackshire J.L., Nondestructive evaluation of aircraft composites using transmissive terahertz time domain spectroscopy, Optics Express, **16**, 17039-17051, 2008.

[10] Wang G, Pran K, Sagvolden G, Havsgard GB, Jensen AE, Johnson GA, Vohra ST. Ship hull structure monitoring using fibre optic sensors. Smart Mater Struct., **10,** 472–8, 2001.

[11] Yashiro S., Takeda N., Okabe T., Sekine H., A new approach to predicting multiple damage states in composite laminates with embedded FBG sensors. Composites Science and Technology, **65,** 659-667, 2005.

[12] Qiu Y., Wang Q.B., Zhao H.T., Chen J.A, Wang Y.Y., Review on composite structural health monitoring based on fiber Bragg grating sensing principle. Journal of Shanghai Jiaotong University (Science), **18**, 129-139, 2013.

[13] Kahandawa G.C., Epaarachchi J., Wang H., Lau K.T., Use of FBG Sensors for SHM in Aerospace Structures. Photonic Sensors, **2**, 203–214, 2012.

[14] Kim S.W., Kang W.R., Jeong M.S., Lee I., Kwon I.B., Deflection estimation of a wind turbine blade using FBG sensors embedded in the blade bonding line, Smart Mater. Struct., **22**, 125004 (11pp), 2013.